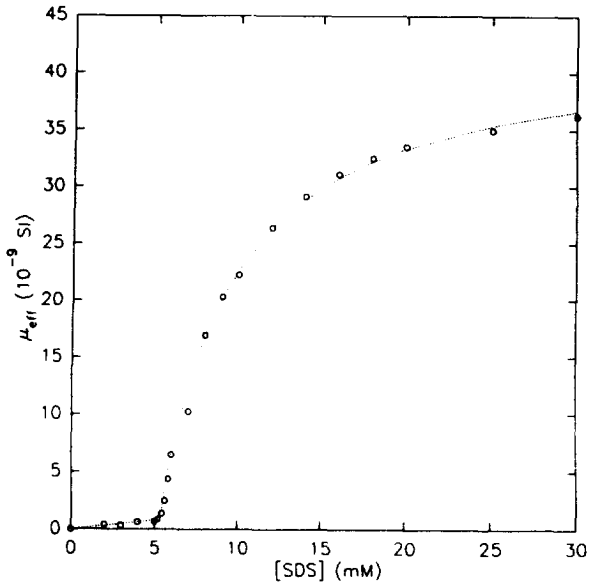

Fig. 6. Comparison between (symbols) the experimental and (line) the theoretical evolution of the electrophoretic mobility of naphthalene as a function of the total SDS concentration. Electrolyte: $5 \cdot 10^{-3}$ mol l^{-1} borax.

analysis of the experimental graph in Fig. 3. Fig. 6 shows a perfect fit between the experimental and the deduced theoretical values, and therefore validates without ambiguity this new technique as a method for the determination of the cmc. Moreover, the so-deduced cmc value ($5.29 \cdot 10^{-3}$ mol l^{-1}) is identical with that reported in the literature [11], using surface tension measurements, under the same experimental conditions (25°C, $[Na^+] = 0.01$ mol l^{-1}). This perfect fit not only from the theoretical but also the experimental point of view confirms capillary electrophoresis as the technique of choice for micellization process studies.

5. Conclusion

The results obtained in this study establish capillary electrophoresis as a preferred technique for the determination of the cmc of anionic surfactants, as it is not only rapid but also easy to carry out and, above all, is readily automatable.

Based on studies of the micellization process in various aqueous solutions, we intend, in the near future, to proceed to the evaluation of the cmc of SDS in various electrophoretic media used in MEKC, i.e., concerning inorganic salts, borax and the sodium salts of phosphoric acid at different concentrations and pH values, and concerning organic solvents, methanol, ethanol, acetonitrile and acetone, which cover a broad lipophilic range and are therefore the most widely employed, either to adjust the aqueous phase lipophilicity, to increase the selectivity of the chromatographic system or to modify the retention time window. Moreover, we shall attempt to widen the fields of application of this technique for the determination of cmc to anionic surfactants with different structures and to cationic and neutral surfactants.

References

[1] P. Mukerjee and K.J. Mysels, Critical Micelle Concentrations of Aqueous Surfactant Systems, NSRDS-NBS 36, National Bureau of Standards, Washington, DC, 1971.
[2] S.A. Swedberg, J. Chromatogr., 503 (1990) 449.
[3] S. Terabe, K. Otsuka and T. Ando, Anal. Chem., 57 (1985) 834.
[4] C. Treiner, Composés Tensioactifs en Solution aqueuse, Phénomènes d'Interface Agents de Surface, Technip, Paris, 1983, Ch. 3.
[5] Y. Walbroel and J.W. Jorgenson, Anal. Chem., 58 (1986) 479.
[6] J.N. Phillips, Trans. Faraday Soc., 51 (1955) 561.
[7] M. Almgren, F. Grieser and J.K. Thomas, J. Chem. Soc., Faraday Trans. 1, 75 (1979) 1674.
[8] H.H. Perkampus, UV-VIS Atlas of Organic Compounds, VCH, Weinheim, 2nd ed., 1992.
[9] E.G. Aniansson and S.N. Wall, J. Phys. Chem., 78 (1974) 1024.
[10] J.C. Jacquier, C. Morin and P.L. Desbène, unpublished results.
[11] D. Stigter, in Physical Chemistry, Enriching Topics for Colloids and Surface Science, IUPAC Commission I.6, Theorex, La Jolla, CA, 1975, Ch. 12.

ELSEVIER

Journal of Chromatography A, 718 (1995) 177–185

JOURNAL OF CHROMATOGRAPHY A

Simple double-beam absorption detection systems for capillary electrophoresis based on diode lasers and light-emitting diodes

Wei Tong, Edward S. Yeung*

Ames Laboratory-U.S.D.O.E. and Department of Chemistry, Gilman Hall, Iowa State University, Ames, IA 50011, USA

First received 4 May 1995; accepted 7 June 1995

Abstract

Simple double-beam absorption detection systems for capillary electrophoresis (CE) based on diode lasers and light-emitting diodes (LEDs) are developed. Using digital normalization, the intensity fluctuations are greatly reduced and a relative standard deviation of the background noise of 10^{-5} to 10^{-6} can be achieved. The detection performance is thus improved over those of commercial CE systems. For the diode-laser-based system, the gain in detectability results from both a reduction in intensity fluctuations and a better optical coupling of the laser beam with the small capillary tube, maximizing the effective optical path length. The improvement in the LED-based system is largely due to the excellent stability of the LED augmented by double-beam cancellation of the baseline fluctuations. Indirect absorption detection for cationic and anionic species are also demonstrated, extending the applicability of the system.

1. Introduction

Capillary electrophoresis (CE) is one of the fastest growing separation techniques today [1,2]. Various detection methods, including absorption, fluorescence, electrochemistry, and mass spectrometry, have been used for CE [3]. Because of their versatility and simplicity, absorption detectors are still the most popular. However, it has been an inherent weakness in absorption detection that the concentration limit of detection (LOD) is poor. This is due to the high background noise level due to low light intensities, the very short optical path length, and the poor optical coupling resulting from the small capillary size. These need to be improved for further development of absorption detection in CE.

Recently, we demonstrated a double-beam laser absorption detection scheme in CE using a novel electronic circuit to reduce the background noise [4]. A practical noise-to-signal ratio of $1 \cdot 10^{-5}$ in intensity is achieved. Further applications of this system were demonstrated for UV-absorption detection [5], indirect absorption detection [6], and high-performance liquid chromatography (HPLC) [7,8]. Diode lasers have the advantage of small size, low cost, and low noise [9]. Recently, diode lasers have been used in fluorescence detection for LC [10] and CE [11,12]. A diode-laser-based absorption detector using a lock-in amplifier was also reported [13]. In the present study, a very simple diode-laser-based double-beam absorption detection system is demonstrated. The two well-correlated laser

* Corresponding author.

0021-9673/95/$09.50
SSDI 0021-9673(95)00638-9

beams reflected from a glass window were used as signal and reference beams, respectively. With a standard A/D interface and subsequent re-normalization, the background fluctuations are largely canceled out. The detectability is improved over commercial double-beam CE systems and is close to that of our previous study with an electronic noise-canceler.

In addition, it is well known that light-emitting diodes (LEDs) are an exceptionally stable light source [14]. Recently, LEDs with ultra-high intensities at a variety of wavelengths (ranging from blue to red, with spectral bandwidth from 20 to 100 nm) have become commercially available from several manufacturers. They have been used as a light source for absorption [15], fluorimetric titration [16], and fluorimetry [17]. However, there have not been any reports using LED as the light source for optical detection in CE. In fact, the combination of extremely high stability, reasonably high intensity, small size, low cost, and very long lifetime makes the LED an attractive source for further improvement of absorption detection in CE. We report here a new absorption detection system based on LED. Despite the difficulty of optical focusing and the poor coupling of the beam with a small-diameter capillary, the detection limit is still close to that of the diode-laser-based system.

Since a large number of analytes lack proper chromophores for UV–Vis detection after CE, indirect absorption detection has been employed as a "universal' approach [18]. Except for a few [6,19] examples, indirect detection schemes in CE are operated in the UV. However, sensitivity and applicability of indirect UV detection can be adversely affected by the absorption of the UV light by analytes and/or by matrix constituents in the sample [19]. For this reason, the application of the present systems for indirect detection in the visible range is also evaluated.

2. Experimental

A schematic diagram of the diode-laser-based double-beam absorption detector for CE is shown in Fig. 1A. The light source was a 10-mW LAS200-670-10 (670 nm) or LAS200-635-10 (635 nm) diode laser (Lasermax, Rochester, NY,

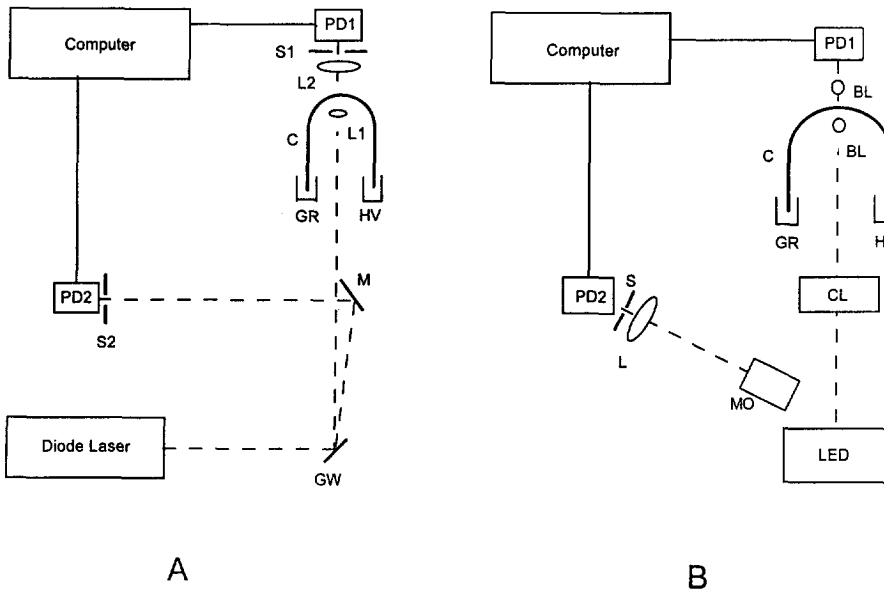

Fig. 1. Experimental setups of double-beam absorption detection for CE. (A) Diode-laser-based system. GW, glass window; M, mirror; S1 and S2, apertures; L1, 1-cm focal length lens; L2, 3.5-cm focal length lens; PD1 and PD2, photodiodes; C, capillary; HV, high-voltage power supply; GR, ground. (B) LED-based system. CL, camera lens; MO, microscope objective; BL, ball lens; S, aperture; L, lens; others are the same as in (A).

USA) powered by a 9-V battery or a home-made power stabilizer. Two photodiodes (BPW34, Siemens) were used as signal- and reference-beam detectors. The laser beam was reflected by the two surfaces of a glass window (BK7). One of the two reflected beams was reflected by a mirror (Newport) and passed through a 5-mm aperture before reaching a photodiode, PD2. The signal beam was focused by a 1-cm focal length lens onto the detection window of the capillary. The capillary was mounted on a precision x–y positioner (Newport, 462 Series) for fine adjustment relative to the focal point. The transmitted signal beam through the capillary was collected by a 3.5-cm focal length lens. After passing through a 5-mm aperture, the signal beam was monitored by a photodiode, PD1. Low-pass (1 Hz) filters were employed at both photodiodes to limit the output bandwidth.

The schematic setup for the LED-based system is shown in Fig. 1B. The source LEDs used were AND130CR (peak wavelength 660 nm) and HLMP-3950 (peak wavelength 565 nm) (Hewlett-Packard). Power was supplied to the LEDs by a 12-V car battery in series with a 500-Ω current-limiting resistor. The d.c. forward current in the LED was 20 mA. The LEDs were "aged" by operating for about a week at 20 mA to eliminate the initial low-frequency noise component that is common to freshly manufactured devices [17]. Unlike the unidirectional laser source, the LEDs have certain view angles (16° for AND130CR and 24° for HLMP-3950), which make them difficult to be focused by conventional lenses. A 24-mm focal length wide-angle camera lens (Tamron, Japan) was used to focus the beam spot down to a diameter of 1 mm. The spot was further focused by a pair of ball lenses from a commercial CE system (Spectraphoresis 1000, Spectra Physics, Mountain View, CA, USA) before reaching the signal detector, PD1. The capillary detection window was positioned between the two ball lenses. PD1 was put very close to the ball lens to collect more light. The reference beam was collected by a microscope objective lens close to the LED and was focused onto the reference detector, PD2, by a lens. The same photodiodes as those in the diode-laser-based system were used for the LED-based system. However, different combinations of resistors and capacitors were used to maintain an RC time constant of 1 s. Signal and reference data were acquired at 5 or 10 Hz by the two channels of a 24-bit A/D conversion interface (ChromPerfect, Justice Innovation, Palo Alto, CA, USA). The data was stored in an IBM/PC-compatible computer for subsequent renormalization.

A high-voltage power supply (Glassman, Whitehouse Station, NJ, USA) was used to supply high voltage across the capillary. A commercial double-beam CE system (Spectraphoresis 1000, Spectra Physics, Mountain View, CA, USA) operated at the same wavelength was used for comparison. The capillaries used for direct detection were fused-silica 75 μm I.D. and 360 μm O.D. (Polymicro Technologies, Phoenix, AZ, USA) with various lengths. The capillaries were flushed with 0.1 *M* NaOH overnight, followed by equilibration with the running buffer for one day. For indirect detection, 50 μm I.D. DB-1 capillaries (J&W Scientific, Folsom, CA, USA) were used. The DB-1 capillaries were equilibrated with the running buffer for one day before use. The sample solutions were injected hydrodynamically by raising the analyte vial 15 cm above the ground buffer reservoir for 7 s. The analytes for indirect detection were dissolved in the running buffer for injection.

The running buffer for direct CE detection was 10 m*M* disodium phosphate (Fisher, Fair Lawn, NJ, USA) at different pHs. The running buffer for indirect CE detection of cations was adapted from Ref. [19], and contained 0.12 m*M* methyl green in 1 m*M* tris(hydroxymethyl)aminomethane (Tris) and 2.5 m*M* acetic acid (pH 3.9). For indirect detection of anions, the running buffer was 20 m*M* permanganate (pH 7.0). Oxazine-1 perchlorate was obtained from Kodak (Rochester, NJ, USA), methyl green (zinc chloride salt) from Aldrich (Milwaukee, WI, USA), malachite green from Exciton (Dayton, OH, USA), Tris from Fisher, and bromothymol blue from J.T. Baker (Philipsburg, NJ, USA). All solutions and buffers were filtered with a 22-μm cutoff cellulose acetate filter before

use. The water was deionized with a water purification system (Millipore, Milford, MA, USA).

3. Results and discussion

3.1. Background noise cancellation

Successful cancellation of background noise can be achieved only if the optical characteristics of the signal and reference channels are truly identical. Therefore, how to split the laser beam to obtain two closely correlated or co-fluctuating beams is an important consideration. The signal beam here passed through a capillary filled with running buffer (10 m*M* phosphate, pH 10.4). Beam splitters, beam displacers and glass windows were examined for this purpose. It was found that the two reflected laser beams from the two surfaces (front and back) of a glass window were the best correlated (Fig. 2A). These two beams are also quite stable, with the residual noise approaching the resolution limit of the A/D board. Therefore, some digitization noise exists. However, the A/D interface (ChromPerfect) used to monitor the beams is actually asynchronous in operation. This can be confirmed by monitoring the same signal from a waveform generator via the two channels. Therefore, simply subtracting or dividing the reference data points from the signal data points does not

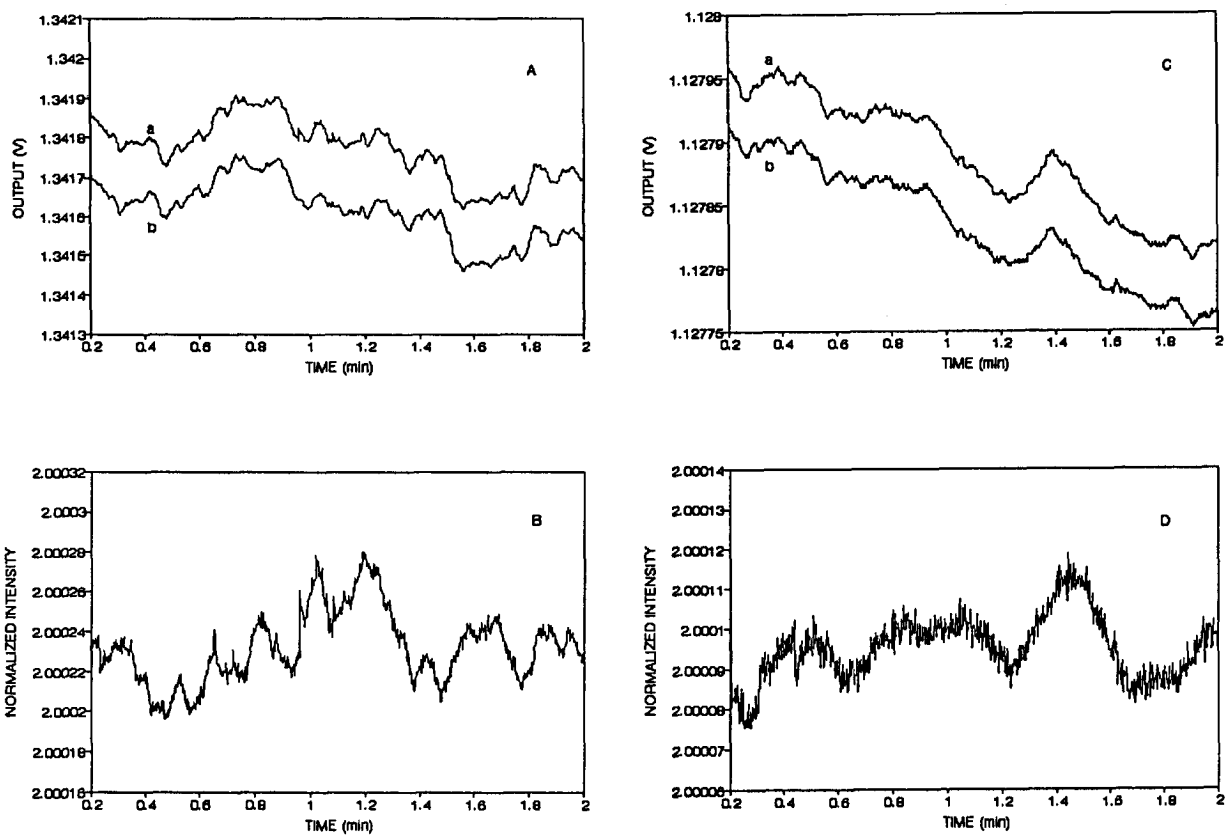

Fig. 2. Background noise of diode laser and LED. (A) Signal (a) and reference (b) beams for diode laser before cancellation. (B) Output intensity of (A) after cancellation by Eq. 1. (C) Signal (a) and reference (b) beams for LED before cancellation. (D) Output intensity of (C) after cancellation by Eq. 1.

give the best cancellation. What we did was to use the sum of the two adjacent data points in channel a (interpolation) and divide that by the data point in channel b to get the normalized output intensity, I:

$$I = (a_i + a_{i+1})/b_i \quad (1)$$

Here a_i and a_{i+1} are the ith and $(i+1)$th data points in channel a, and b_i is the ith data point in channel b. This has an averaging effect and the resulting background noise showed a relative standard deviation of $1 \cdot 10^{-5}$. The high-resolution A/D conversion is critical here. The residual peaks observed in Fig. 2B were most likely due to the asynchronous movements of the optical components for the two beams. So, the ruggedness of the setup is very important. From another point of view, this also proves that the proposed cancellation scheme is suitable for cancellation of correlated noise components. With this simple system (Fig. 1), the possibility of mechanical movements can be reduced compared to a complicated setup. He–Ne and Ar lasers were also tested with the same setup. The cancellation results were less impressive. This is largely due to the inherent instability of these laser systems. One needs to account for the higher-frequency fluctuations by sampling the two beams at a higher rate for proper cancellation.

For the LED-based system, obtaining the signal and reference beams is not so easy. Many beam-splitting techniques do not apply simply because the beam from the LED is not unidirectional, like the laser beam. In this case, the reference beam is collected by putting a microscope objective very close to the LED. The two beams thus obtained are also quite well correlated (Fig. 2C). Since the LED appears to be more stable but is at a lower intensity than the diode laser, there is more digitization noise before (Fig. 2C) and after (Fig. 2D) cancellation. Despite this, the background noise still has a relative standard deviation of only $3.6 \cdot 10^{-6}$. As we will discuss later, this noise can be further eliminated by averaging and smoothing after normalization.

3.2. Direct absorption detection

As a demonstration, the separation of oxazine-1 and bromothymol blue was performed in our diode-laser system (Fig. 3). The baseline is stable and the peaks are sharp, indicating the lack of broadening due to the detector. When the concentration of oxazine-1 was reduced ($6.7 \cdot 10^{-8}$ M) to approach its detection limit, the peak was hardly distinguishable from the background noise (Fig. 4A) if merely the signal-channel data is plotted (e.g., single beam). However, after our double-beam renormalization scheme the oxazine-1 peak is several times above the background noise level (Fig. 4B). This shows the effectiveness of this noise-cancellation technique.

The absorbance of an analyte in CE should be predictable from Beer's law. For small absorbance, Beer's law can be written as:

$$|\Delta I|/I_0 = 2.303\epsilon bc = 2.303A \quad (2)$$

where $|\Delta I|$ is the absolute intensity change caused by absorption, I_0 is the initial intensity without analyte, ϵ is the molar absorptivity of the analyte, b is the optical path length, c is the analyte concentration, and A is the absorbance

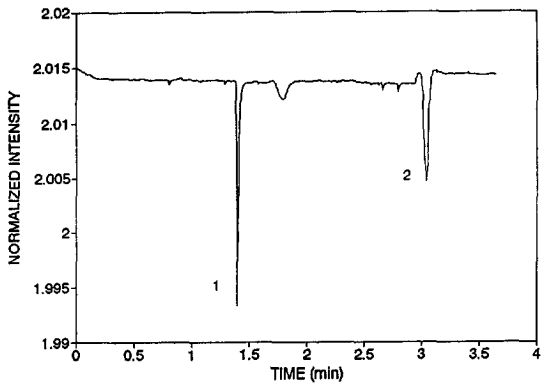

Fig. 3. Electropherogram of a mixture of oxazine-1 (1) and bromothymol blue (2) with injected concentrations of $7 \cdot 10^{-6}$ and $2 \cdot 10^{-5}$ M, respectively. The running potential was 18 kV. The running buffer was 10 mM phosphate at pH 10.4. A 75 μm I.D., 360 μm O.D. capillary with 50 cm total length and 38 cm to the detector was used.

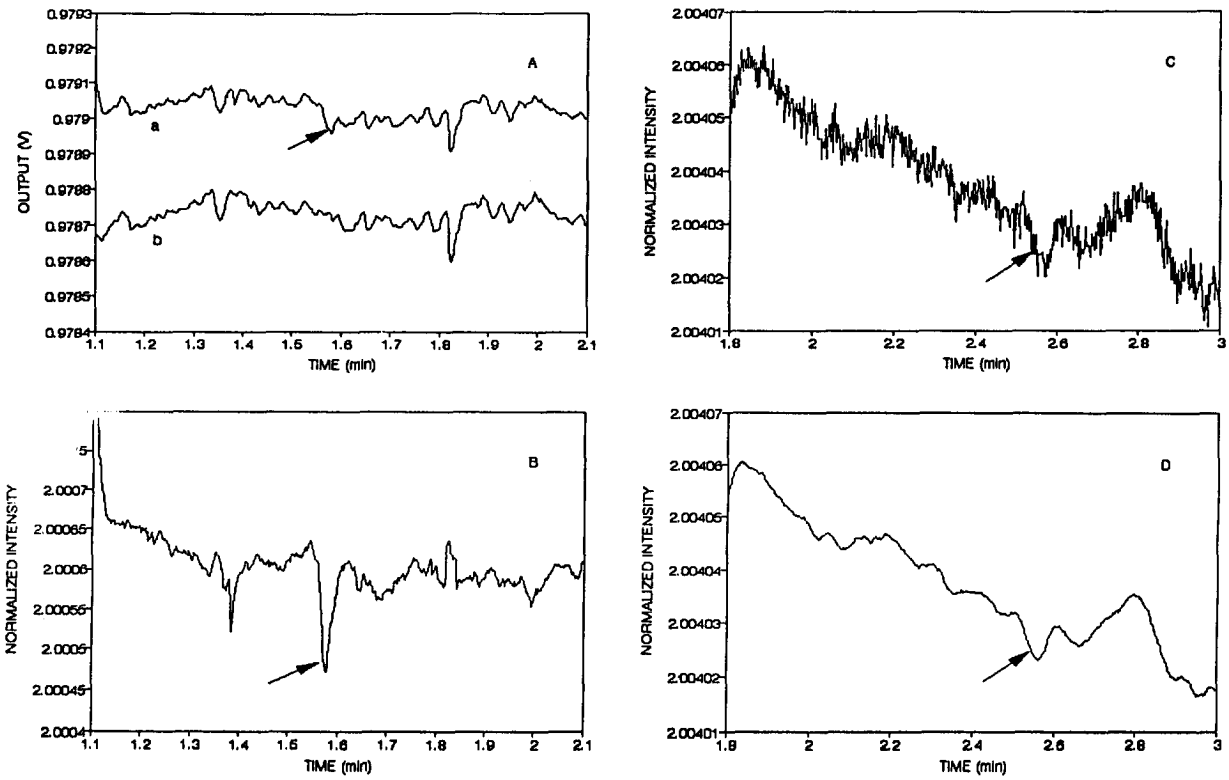

Fig. 4. Electropherogram of $6.7 \cdot 10^{-8}$ *M* oxazine-1 (injected). For (A) and (B), the diode-laser-based system was used and the conditions were the same as those in Fig. 3. (A) Raw data of signal channel before cancellation, and (B) after cancellation. For (C) and (D), the LED-based system was used. The running potential was 20 kV and the capillary length was 70 cm total and 55 cm to the detector. Other conditions were the same as those in Fig. 3. (C) After cancellation, (D) data in (C) after ten-point box-car smoothing.

of the analyte in the capillary. In our diode-laser-based system, the capillary was inclined 30° from the vertical direction to minimize multiple reflection. The actual optical path length is therefore 87 μm. The molar absorptivity of oxazine-1 at pH 10.4 was measured in a spectrometer to be $6.43 \cdot 10^4$ l mol^{-1} cm^{-1}. According to Beer's law, the theoretical absorbance of $6.7 \cdot 10^{-8}$ *M* of oxazine-1 in the capillary is $3.75 \cdot 10^{-5}$. From Fig. 4B, ΔI for oxazine-1 is about $1.7 \cdot 10^{-4}$ and I_0 is about 1.99. From Eq. 2, the absorbance, *A*, is calculated to be $3.7 \cdot 10^{-5}$, which matches the theoretical value very well. This means that the laser beam passed through the center of the capillary and the full diameter of the capillary was utilized as the optical path length. This is actually not surprising because the laser beam can be focused down to a few micrometers and superior optical coupling can be achieved easily. However, in the LED-based CE system such coupling cannot be realized because of the limitations of the light source. Fig. 4C is the electropherogram of $6.7 \cdot 10^{-8}$ *M* oxazine-1 from the LED-based CE system. After ten-point smoothing, the oxazine-1 peak is more clearly visible (Fig. 4D). But this peak height is not predicted by Beer's law. This shows that the beam did not all pass through the diameter of the capillary. Since the LED appears to be more stable than the diode laser, the background noise level is lower in the LED-based CE system. This results in a similar detection limit to that of the diode-laser-based system. However, with LEDs we have a better choice of wavelengths suitable for

different analytes, from blue to red in the visible range. LEDs are also less expensive. For the same reason as for LEDs, the peak heights from the commercial system are also not predicted by Beer's law. Fig. 5 is the electropherogram of $2 \cdot 10^{-7}$ *M* oxazine-1 from the commercial CE system. The absorbance observed here is only $3 \cdot 10^{-5}$. Better focusing in the diode-laser system accounts for about four times improvement in the absorbance measured. This effect will be even more dramatic for smaller-diameter capillaries [6].

In our previous study, $2 \cdot 10^{-8}$ *M* malachite green was detectable at 632.8 nm (He–Ne laser) with an electronic noise-canceler [4]. In the simple system reported here, $7 \cdot 10^{-8}$ *M* of injected malachite green also gives good signal-to-noise ratio at 635 nm (diode laser), which is very close to 632.8 nm. But the whole scheme is simplified and the requirements are much less critical. Again, this result is well predicated by Beer's law.

3.3. Indirect detection

For practical applications, the 635 and 670 nm wavelengths provided by the diode laser are not broadly useful. Even with LEDs, which can cover most of the visible range, the wavelengths are still long compared to most chromophores. Fortunately, the same system is applicable to universal detection via indirect absorption as well [6]. Fig. 6A is the electropherogram of several cations obtained by the diode-laser-based system. From our previous study, the limit of detection (LOD) for indirect absorption detection can be written as:

$$LOD = \Delta A/[(TR)\epsilon b] \quad (3)$$

where ΔA is the absorbance noise, ϵ is the molar absorptivity of the background chromophore,

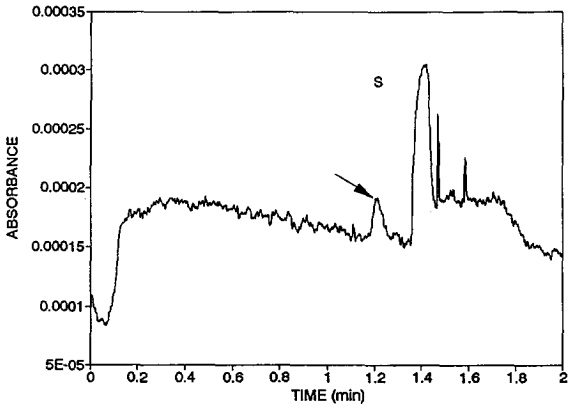

Fig. 5. Electropherogram of $2 \cdot 10^{-7}$ oxazine-1 (injected) from a commercial CE system. The running potential was 15 kV. The total and effective lengths of the capillary were 44 and 35 cm, respectively. Other conditions were the same as in Fig. 3. S, system peak.

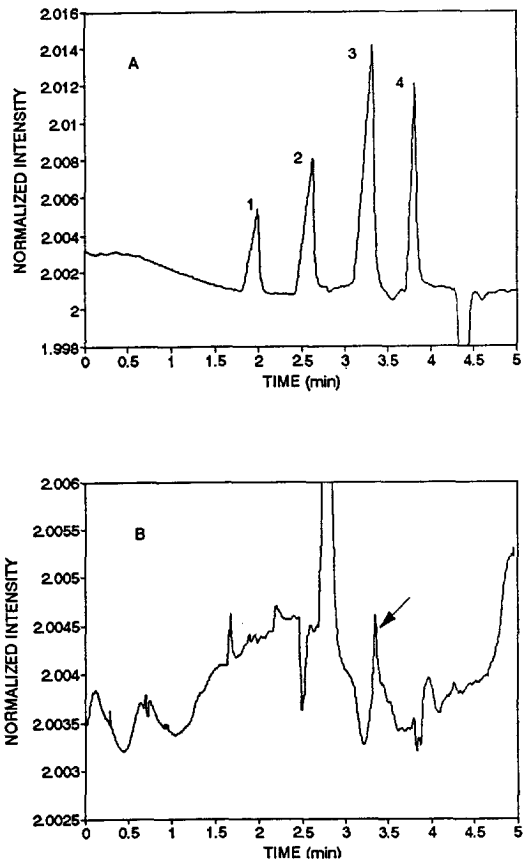

Fig. 6. Electropherograms for the indirect detection of cations in the diode-laser-based system. The running buffer was 0.12 m*M* methyl green in 1.0 m*M* Tris and 2.5 m*M* acetic acid (pH 3.9). The applied potential was 28 kV. A 50 μm I.D. DB-1 capillary with 55 cm total length and 40 cm to the detector was used. (A) Separation of cations (1, $5.2 \cdot 10^{-4}$ *M* K^+; 2, $3.2 \cdot 10^{-4}$ *M* Ca^{2+}; 3, $9.6 \cdot 10^{-5}$ *M* Na^+; and 4, $8.8 \cdot 10^{-5}$ *M* Li^+). (B) Detection limit of Li^+ ($3.5 \cdot 10^{-6}$ *M*).